Available online at www.jourcc.com

Journal homepage: www.JOURCC.com

Journal of Composites and Compounds

Synthesis and characterization of the novel 80S bioactive glass: bioactivity, biocompatibility, cytotoxicity

Ameneh Bakhtiari [a], Amir Cheshmi [b], Maryam Naeimi [c], Sobhan Mohammadi Fathabad [d], Maryam Aliasghari [e], Amir Modarresi Chahardehi [f], Sahar Hassani [g], Vahideh Elhami [h]*

[a] *Department of Biology, Shahid Chamran University, Ahvaz, Iran*

[b] *Department of Materials Engineering, Babol Noshirvani University of Technology, Shariati Avenue, Babol, Iran*

[c] *School of Nursing and Midwifery, Tehran University of Medical Science, Tehran, Iran*

[d] *Department of Engineering and High-Tech, Iran University of Industries and Mines, Tehran, Iran*

[e] *Young Researchers and Elite Club, Yadegar-e-Imam Khomeini (RAH) Shahr-e-Rey Branch, Islamic Azad University (IAU), Tehran, Iran*

[f] *Integrative Medicine Cluster, Advanced Medical and Dental Institute, Universiti Sains Malaysia, Bertam, 13200, Kepala Batas, Penang, Malaysia*

[g] *Department of Cellular and Molecular Biology, Facaulty of Advanced Science and Technology, Tehran Medical Sciences, Islamic Azad University, Tehran, Iran*

[h] *Sustainable Process Technology Group, Faculty of Science and Technology, University of Twente, Drienerlolaan 5, Enschede 7522 NB, The Netherlands*

ABSTRACT

In this research, the 80S bioactive glass with different Ca/P ratios was prepared by the sol-gel route. Scanning electron microscopy (SEM), transmission electron microscopy (TEM), energy dispersive spectroscopy (EDS), X-ray diffraction (XRD), and Fourier transforms infrared spectroscopy (FTIR) were used to study the apatite structure and shape. According to the results, the $78SiO_2$–$17P_2O_5$–5CaO bioglass showed a higher rate of crystalline hydroxyapatite (HA) on its surface in comparison with the other bioglasses. After 3 days of immersion in the SBF solution, spherical apatite was formed on the $78SiO_2$–$17P_2O_5$–5CaO surface, which demonstrated high bioactivity. A statistically significant promotion in proliferation and differentiation of G292 osteoblastic cells was also observed. Regarding its optimal cell viability and bioactivity, the $78SiO_2$–$17P_2O_5$–5CaO bioactive glass could be offered as a promising candidate for bone tissue applications.

Peer review under responsibility of JCC Research Group

ARTICLE INFORMATION

Article history:
Received 17 May 2020
Received in revised form 03 July 2020
Accepted 29 August 2020

Keywords:
Bioactive glass
80S
Ca/P ratio
Hydroxyapatite

1. Introduction

As a result of bone infections, cancer removal, an injury, or other disease, millions of people suffer from bone failure or loss annually. Bone is able to repair itself when damages are minor, however, in the case of pathological fractures or massive defects, it fails to regenerate [1, 2]. In these cases, most common therapy techniques are permanent implants or implantation of bone grafts. The main drawbacks of the commonly applied methods in bone surgery include corrosion and cytotoxicity of metallic objects, shortage of donors, wearing of synthetic materials, and risk of infection in transplantation cases [3-6].

Glass materials play a significant role in permanent and biodegradable implants [7, 8]. Due to their ability to form HA as the main mineral of bone, BGs are suitable materials to be used for bone regeneration [9, 10]. They also can create a strong bond with both soft tissues and bone, and hence their osteoconductivity has been proven [11-13]. BGs are particularly advantageous for repair and replacement of damaged bone in tissue engineering, owing to their high bioactivity and biocompatibility [14, 15].

BGs mainly contain P_2O_5, SiO_2, and CaO enabling a HA layer formation on their surfaces. This layer improves the binding of BGs with bones. SiO_2 is an important network forming constituent in the glass structures [16]. Furthermore, it is able to promote the cell functions by releasing Si ions into cell culture media, and nucleation of calcium phosphate phase is facilitated by P_2O_5 on the glass surface [5, 6].

Since 1991 when a sol-gel method was developed for the synthesis of bioactive glasses, various compositions of glass samples have been produced by this technique at low temperatures [17-19]. Various bioactive compositions can be prepared to achieve great degradation/resorption behavior and bone-bonding rates because of the high porosity and surface area of the prepared sol-gel glasses [20-22]. Using the sol-gel processing routes for the production of BGs has been suggested by previous investigations and it has been reported that the production of novel BGs with a variety of chemical compositions is possible [11, 23, 24].

Lin et al. [20] prepared $80SiO_2$–$15CaO$–$5P_2O_5$ glass powders by the

* *Corresponding author:* Amir Modarresi Chahardehi*; E-mail:* amirmch@gmail.com

DOR: 20.1001.1.26765837.2020.2.4.1.3
https://doi.org/10.29252/jcc.2.3.1

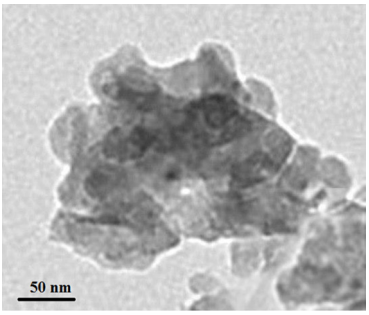

Fig. 1. TEM image the powders after the preparation by the sol-gel route.

sol-gel method. They found that mixing phosphoric acid (PA) with the glass powders exhibited positive effects on the decrease of the dentin penetration and occlusion of the dentinal tubule. Mixing 80S-BG with appropriate PA demonstrated good operability and short reaction time, which makes it feasible to occlude dentinal tubules.

This research aims to prepare 80S BGs with different Ca/P ratios via a sol-gel method. Subsequently, the formation of the hydroxyapatite on the surfaces of the bioactive glass is evaluated using the XRD, FTIR, SEM, and EDX analyses. The potential of the samples in cell proliferation is also studied.

2. Materials and Methods

2.1. Materials

To synthesize the bioactive glasses, calcium nitrate tetrahydrate ($Ca(NO_3)_2{\cdot}4\,H_2O$), Triethyl phosphate (TEP, $(C_2H_5)_3PO_4$), and Tetraethyl orthosilicate (TEOS, $Si(OCH_2CH_3)_4$) with high analytical grades were used. All materials were obtained from Merck Company.

2.2. Synthesis of bioactive glass

The composition of the studied 80S-BGs were 78% SiO_2-17% CaO-5%P_2O_5 (BG-5P), 78% SiO_2-16% CaO-6%P_2O_5 (BG-6P), and 78% SiO_2-18% CaO-4%P_2O_5 (BG-4P) in mol.%. To synthesize the samples, TEP, $Ca(NO_3)_2.4H_2O$, and TEOS were dissolved at room temperature. TEOS was first mixed with nitric acid to obtain a diluted and clear solution. Under constant stirring, calcium nitrate and TEP were then added to the solution. The addition of reagents was carried out sequentially and the time for the complete reaction of each reagent was 40 min. To form the gel, the mixture was stored at room temperature for 9 days in closed containers. Drying of the formed gel was conducted in two stages at 80 °C for 72 h and 130 °C for 24 h. In order to eliminate residual nitrate and all organic substances, the dried material was heated to 750 °C for 2 h.

2.3. Bioactive glass Characterizations

2.3.1. TEM analysis

One of the applicable tools for the analysis of the nanomaterial microstructure is TEM. In this research, to study the obtained glass particles, TEM (CM200-FEG-Philips) with the acceleration voltage of 200 kV was employed. To observe the glass particles, the particles were deposited on Cu support grids from a dilute suspension in ethanol.

2.3.2. XRD analysis

The determination of the formed phases in BG and HA structures was carried out by X-ray diffraction (INEL Equinox 3000) in 2θ between 20° to 90° using the CuKα radiation. The characteristics of the analysis were tube electric current=30 mA, tube voltage=40 kV, scanning speed = 2°/min, and wavelength λ=1.540510 Å.

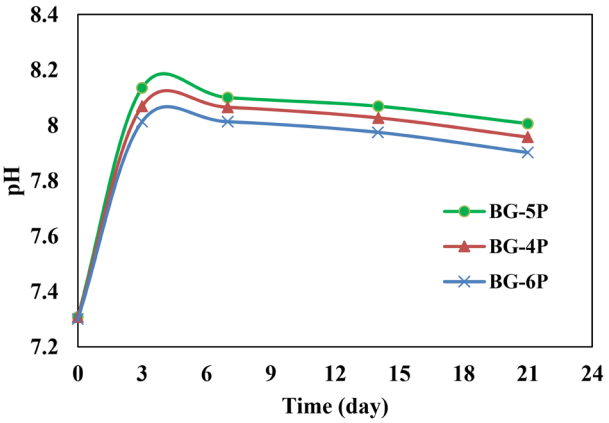

Fig. 2. Change of pH during 21 days of soaking in SBF.

2.3.3. FTIR analysis

To evaluate the formation of hydroxyapatite, FTIR spectrometer (Bomem MB 100) was employed to determine the functional groups present in glass powders. The powders were blended with potassium bromide (KBr) while the blending ration was 1:9. Using a hand press, discs with the diameters less than 6 mm were produced from the blended powders. Recording of FTIR wave numbers was performed in the range of 4000 to 400 cm^{-1}.

2.3.4. MTT assay

To study the biocompatibility of BGs, the proliferation of G292 osteoblastic cells on the samples was studied by 3-(4, 5-dimethylthiazol-2-yl)-2, 5-diphenyltetrazolium bromide (MMT) assay. The cell line was obtained from Pasteur Institute (the National Cell Bank of Iran). Cell culture was performed under standard culturing conditions and the cultured cells were maintained in 90% moisture for 24 h at 37 °C. A 96-well plate was used for seeding the cells. The cultured osteoblastic cells were seeded at a density of 6×10^3 cells/well and maintained for 1 day for attachment. The related absorbance measurements were carried out at a wavelength of 570 nm with a multi-well microplate reader (BioTek Instruments). Three readings were done for each specimen.

2.3.5. Simulated body fluid (SBF)

One of the easiest methods for the biomineralization study of BGs is the SBF test. It is also quick and cost-effective. This test can appropriately simulate the osteo-production conditions, which exist in osseous tissue. Also, it is suitable for bioactivity investigation of materials and the contributing bone-bonding mechanisms [5]. The ionic concentration and composition of SBF are similar to human body plasma (Na_2HPO_4, Na_2SO_4, $CaCl_2$, HCl, $MgCl_2$, KCl, $NaHCO_3$, NaCl, and $(CH_2OH)_3(CNH)_2$ as the buffering agent). The prepared solution buffered at 37 ˚C with 1 N HCl solution and TRIS (trishydroxymethylaminomethane) at pH = 7.25. The 80S bioactive glass powders were immersed in the prepared SBF at 37˚C for 3, 7, and 14 days. The concentration of the immersed powders was 1.5 mg of powder per milliliter of the solution. The powders were filtered and dried after the determined time.

2.3.6. SEM-EDS

SEM and EDS were employed for the evaluation of the composition and morphology of the bioactive glasses before and after the bioactivity tests. The reaction between the solution and bioglass powders resulting in the surface evolution was studied. The acceleration voltage was 15 kV and the samples were gold-coated before the analysis.

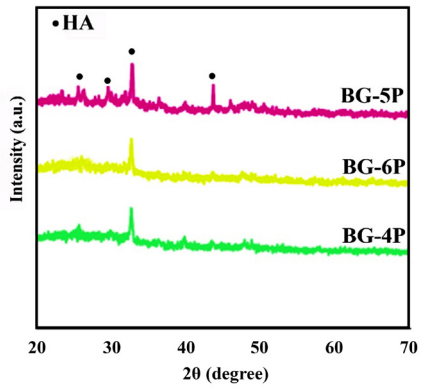

Fig. 3. XRD patterns of BGs after soaking in SBF for 21 days.

3. Result and discussion

3.1. TEM analysis of as-prepared samples

Fig. 1 depicts the TEM image of the as-prepared powder of BG-5P. The TEM image shows the formation of bioactive glass nanoparticles with the irregular-round shape. The diameter of the nanoparticles is between 40 to 60 nm.

3.2. pH analysis

Fig. 2 illustrates the changes in the pH value of SBF during 21 days of soaking. According to the literature, the pH evaluation of the SBF solution after the immersion can determine the process of HA formation. A similar trend was observed for all the samples. As seen, a remarkable increase in pH occurred for the BG-5P after 7 days. It indicated that cationic ions dissolved in the solution from the surface of BG. The silica network of the glass was attacked by the solution at high pH. After 7 days of immersion, the pH started to decrease revealing the absorption of calcium and phosphate ions from SBF. Therefore, it demonstrates the increase in hydroxyapatite formation on the surface of BGs.

3.3. XRD analysis

After 21 days of soaking, the structure of BGs was studied by XRD and the results are presented in Fig. 3. As illustrated, the peaks attributed to the presence of crystalline HA were observed. The diffraction peaks at 2θ of 32° are related to the (211) plane of crystalline hydroxyapatite confirming the formation of HA on the samples after 21 days of soaking in SBF. Moreover, the intensity of this peak is higher in BG-5P in comparison with other samples indicating the higher tendency of BG-5P to form hydroxyapatite on the glass surface. This might be due to the Ca/P ration. In this bioglass, this ratio is 1.7, which is close to the Ca to P

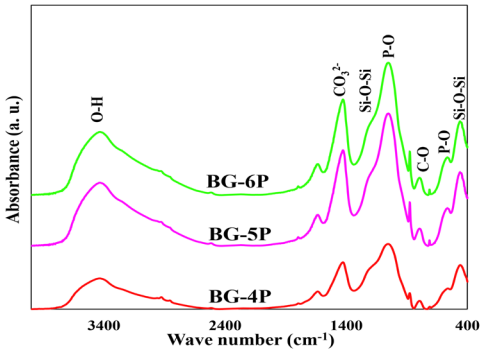

Fig. 5. FTIR spectra for bioactive glass powders after immersion in SBF.

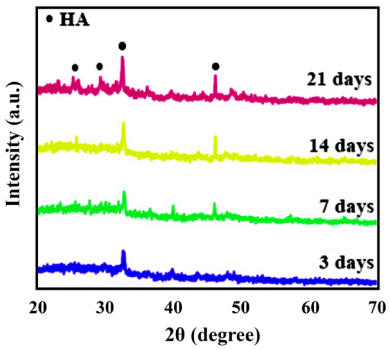

Fig. 4. XRD patterns of BG-5P after soaking in SBF for 3, 7, 14, and 21 days.

ratio in the structure of human bone. The similar intensity was observed for BG-4P and BG-6P. Fig. 4 demonstrates the XRD patterns of BG-5P after soaking in SBF for 3, 7, 14, and 21 days of immersion in the SBF solution. As seen, the intensity of the peaks related to the formation of crystalline HA increased with the soaking time showing that more hydroxyapatite crystals were formed on the samples' surface.

3.4. FTIR analysis

Figs. 5 and 6 illustrate the FTIR spectra of the bioactive glasses after 14 days of immersion and Fig. 5 depicts the FTIR spectra of BG-5P during 14 days. As shown, two peaks appeared at 1455 and 870 cm^{-1} after 3 days. These peaks are related to carbonate (C–O stretching) groups. The spectra of BG-4P, BG-5P, and BG-6P showed Si-O bending vibration band at 476 cm^{-1}, Si-O symmetric stretching band at 798 cm^{-1}, Si-O-Si asymmetric stretching band at 1000–1250 cm^{-1}, C-O group asymmetric bending vibration band at 874 cm^{-1}, and C=O asymmetric stretching bands at 1652 cm^{-1}. Peaks appeared at 568 and 602 cm^{-1} show the bending vibrations of P–O bonds related to the crystalline hydroxyapatite in all glass samples. The wavenumbers of 1056, 605, and 565 cm^{-1} reveal P–O bending vibrations. Amorphous hydroxyapatite is presented by the broad bands around 1056 cm^{-1} attributed to P–O bending vibrations. The obtained results exhibit the HA growth on the surfaces of the bioactive glasses. The intensity of the peaks is higher in BG-5P revealing the higher amount of HA formation on the surface of the glass. The spectra obtained from the glass in Fig. 6 exhibits that the amount of HA increased by increasing the soaking time.

3.5. Morphology of HA

Fig. 7 illustrates SEM micrographs of the bioglass samples after 21 days of immersion. Full coverage of the surfaces with HA crystals can be observed for all the samples after 21 days. The formation of HA on the bioglasses was also confirmed by the FTIR and XRD analyses. Fig. 7a shows the irregular shape of HA phase, while the hydroxyapatite crystals on BG-5P had both irregular and spherical shapes. The HA layer on BG-6P has mostly spherical shapes. The HA crystals show smaller size and

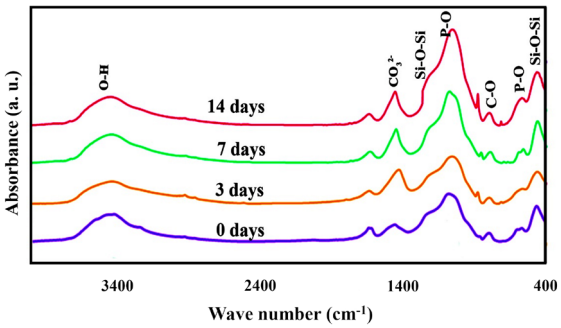

Fig. 6. FTIR spectra of BG-5P after immersion in SBF.

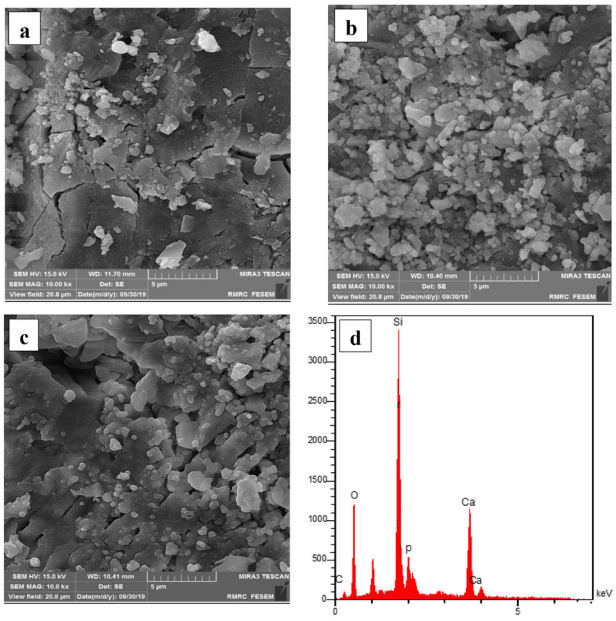

Fig. 7. FSEM images of the glass samples after immersion for 21 days; a) BG-4P, b) BG-5P, c) BG-6P, and d) EDX analysis of BG-5P.

higher dispersity compared to other samples.

EDX analysis of BG-5P after immersion in SBF for 21 days is demonstrated in Fig. 7d. It is confirmed that hydroxyapatite has been successfully formed on the surface of BG-5P.

3.6. Cell viability

Fig. 8 shows the results of the viability test during 7 days. The results indicated that not only the bioactive glass samples were not toxic but also enhanced the cell growth. The cell growth increases by the culturing time for all the samples. However, the BG-5P exhibited higher cell growth compared to the other BGs. This could be due to the optimal Ca/P the sample close to the ratio of human bone. Various biological processes, such as cellular chemotaxis, apoptosis, and differentiation are regulated by extracellular calcium and a calcium-sensing receptor (CaSR). Several studies have indicated that the stimulation of collagen synthesis and proliferation is mostly related to Si contact. Thus, it could be assumed that Si plays a significant role in stimulating angiogenesis, while Ca just helps this process [25].

4. Conclusions

In this research, 80S bioactive glasses with different Ca/P ratios were synthesized using the sol-gel route. The formation of the hydroxyapatite layer was confirmed by the FTIR and XRD analyses after soaking in SBF for all the samples. The results showed that the HA formation rate of BG-5P was higher in comparison with the other two samples. This might be due to the optimum Ca to P ratio close to the Ca to P ratio in human bone composition. The SEM images illustrated the formation of the hydroxyapatite layer on the surfaces of all bioglass samples after immersion for 21 days. The results showed a denser layer with smaller size crystals for BG-5P. Significant cell growth was observed in the MTT in vitro test, while the highest cell viability was related to BG-5P. The results offer this bioactive glass as a promising material for repairing bone defects.

Acknowledgments

The authors received no financial support for the research, authorship and/or publication of this article.

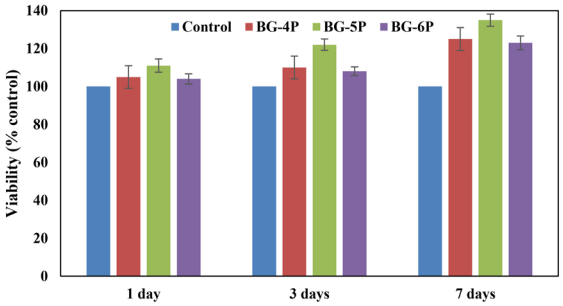

Fig. 8. Cell viability of the bioactive glasses during 7 days.

Conflict of Interest

All authors declare no conflicts of interest in this paper.

REFERENCES

[1] L. Bazli, H. Nargesi khoramabadi, A. Modarresi Chahardehi, H. Arsad, B. Malekpouri, M. Asgari Jazi, N. Azizabadi, Factors influencing the failure of dental implants: A Systematic Review, Composites and Compounds 2(1) (2020).

[2] A. Esmaeilkhanian, F. Sharifianjazi, A. Abouchenari, A. Rouhani, N. Parvin, M. Irani, Synthesis and characterization of natural nano-hydroxyapatite derived from turkey femur-bone waste, Applied biochemistry and biotechnology 189(3) (2019) 919-932.

[3] A. Chlanda, P. Oberbek, M. Heljak, E. Kijeńska-Gawrońska, T. Bolek, M. Gloc, Ł. John, M. Janeta, M.J. Woźniak, Fabrication, multi-scale characterization and in-vitro evaluation of porous hybrid bioactive glass polymer-coated scaffolds for bone tissue engineering, Materials Science and Engineering: C 94 (2019) 516-523.

[4] E. Sharifi Sedeh, S. Mirdamadi, F. Sharifianjazi, M. Tahriri, Synthesis and evaluation of mechanical and biological properties of scaffold prepared from Ti and Mg with different volume percent, Synthesis and Reactivity in Inorganic, Metal-Organic, and Nano-Metal Chemistry 45(7) (2015) 1087-1091.

[5] S. Rahimi, F. SharifianJazi, A. Esmaeilkhanian, M. Moradi, A.H.S. Samghabadi, Effect of SiO_2 content on Y-TZP/Al_2O_3 ceramic-nanocomposite properties as potential dental applications, Ceramics International (2020).

[6] S. Nasibi, K. Alimohammadi, L. Bazli, S. Eskandarinezhad, A. Mohammadi, N. Sheysi, TZNT alloy for surgical implant applications: A Systematic Review, Journal of Composites and Compounds 2(3) (2020) 61-67.

[7] L. Bazli, B. Eftekhari Yekta, A. Khavandi, Preparation and Characterization of Sn-Containing Glasses for Brachytherapy Applications, Transactions of the Indian Ceramic Society 76(4) (2017) 242-246.

[8] F. Sharifianjazi, A.H. Pakseresht, M.S. Asl, A. Esmaeilkhanian, H.W. Jang, M. Shokouhimehr, Hydroxyapatite consolidated by zirconia: applications for dental implant, Journal of Composites and Compounds 2(1) (2020) 26-34.

[9] Z. Goudarzi, A. Ijadi, A. Bakhriari, S. Eskandarinezhad, N. Azizabadi, M.A. Jazi, Sr-doped bioactive glasses for biological applications, Journal of Composites and Compounds 2(3) (2020) 105-109.

[10] J. Daraei, Production and characterization of PCL (Polycaprolactone) coated TCP/nanoBG composite scaffolds by sponge foam method for orthopedic applications, Journal of Composites and Compounds 2(1) (2020) 45-50.

[11] Z. Goudarzi, N. Parvin, F. Sharifianjazi, Formation of hydroxyapatite on surface of SiO_2– P_2O_5–CaO–SrO–ZnO bioactive glass synthesized through sol-gel route, Ceramics International 45(15) (2019) 19323-19330.

[12] F. Sharifianjazi, N. Parvin, M. Tahriri, Formation of apatite nano-needles on novel gel derived SiO_2-P_2O_5-CaO-SrO-Ag_2O bioactive glasses, Ceramics International 43(17) (2017) 15214-15220.

[13] K. Zhang, Q. Van Le, Bioactive glass coated zirconia for dental implants: a review, Journal of Composites and Compounds 2(1) (2020) 10-17.

[14] F. Sharifianjazi, N. Parvin, M. Tahriri, Synthesis and characteristics of sol-gel bioactive SiO_2-P_2O_5-CaO-Ag_2O glasses, Journal of Non-Crystalline Solids 476 (2017) 108-113.

[15] M.S.N. Shahrbabak, F. Sharifianjazi, D. Rahban, A. Salimi, A comparative investigation on bioactivity and antibacterial properties of sol-gel derived 58S bioactive glass substituted by Ag and Zn, Silicon 11(6) (2019) 2741-2751.

[16] F. Sharifianjazi, M. Moradi, A. Abouchenari, A.H. Pakseresht, A. Esmaeilkhanian, M. Shokouhimehr, M.S. Asl, Effects of Sr and Mg dopants on biological and mechanical properties of SiO_2–CaO–P_2O_5 bioactive glass, Ceramics International (2020).

[17] F. Sharifianjazi, A.H. Pakseresht, M. Shahedi Asl, A. Esmaeilkhanian, H. Nar-

gesi khoramabadi, H.W. Jang, M. Shokouhimehr, Hydroxyapatite Consolidated by Zirconia: Applications for Dental Implant, Composites and Compounds 2(1) (2020).
[18] A. Moghanian, A. Ghorbanoghli, M. Kazem-Rostami, A. Pazhouheshgar, E. Salari, M. Saghafi Yazdi, T. Alimardani, H. Jahani, F. Sharifian Jazi, M. Tahriri, Novel antibacterial Cu/Mg-substituted 58S-bioglass: Synthesis, characterization and investigation of in vitro bioactivity, International Journal of Applied Glass Science (2019) 1-14.
[19] L. Bazli, M. Siavashi, A. Shiravi, A Review of Carbon nanotube/TiO_2 Composite prepared via Sol-Gel method, Journal of Composites and Compounds 1(1) (2019) 1-12.
[20] W.-T. Lin, J.-C. Chen, Y.-C. Hsiao, C.-J. Shih, Re-crystallization of silica-based calcium phosphate glass prepared by sol–gel technique, Ceramics International 43(16) (2017) 13388-13393.
[21] J.R. Jones, Reprint of: Review of bioactive glass: From Hench to hybrids, Acta Biomaterialia 23 (2015) S53-S82.
[22] J. Pawlik, M. Widziołek, K. Cholewa-Kowalska, M. Łączka, A.M. Osyczka, New sol-gel bioactive glass and titania composites with enhanced physico-chemical and biological properties, Journal of Biomedical Materials Research Part A 102(7) (2014) 2383-2394.
[23] J.P. Fan, P. Kalia, L. Di Silvio, J. Huang, In vitro response of human osteoblasts to multi-step sol–gel derived bioactive glass nanoparticles for bone tissue engineering, Materials Science and Engineering: C 36 (2014) 206-214.
[24] R.C. Bielby, I.S. Christodoulou, R.S. Pryce, W.J.P. Radford, L.L. Hench, J.M. Polak, Time- and Concentration-Dependent Effects of Dissolution Products of 58S Sol–Gel Bioactive Glass on Proliferation and Differentiation of Murine and Human Osteoblasts, Tissue Engineering 10(7-8) (2004) 1018-1026.
[25] C. Mao, X. Chen, G. Miao, C. Lin, Angiogenesis stimulated by novel nanoscale bioactive glasses, Biomedical materials 10(2) (2015) 025005.